



# An Organotrifluoroborate for Broadly Applicable One-Step <sup>18</sup>F-Labeling\*\*

Zhibo Liu, Maral Pourghiasian, Mark Alex Radtke, Joseph Lau, Jinhe Pan, Gemma M. Dias, Donald Yapp, Kuo-Shyan Lin, Francois Bénard, and David M. Perrin\*

**Abstract:** A new zwitterionic organotrifluoroborate is appended to three radiosynthons that afford undergo facile bioconjugation to several clinically relevant peptides and one enzyme inhibitor. Molecularly complex bioconjugates are <sup>18</sup>F-labeled in a single aqueous step in rapid time (<15 min) without HPLC purification to afford tracers in good yields (>200 mCi, 20–40 %) at high specific activity (≥3 Ci/μmol) and at >98 % purity. PET imaging shows in vivo stability and tumor uptake.

**P**ositron emission tomography (PET) is an imaging technique for preclinical target validation and clinical cancer diagnosis.<sup>[1]</sup> Of the many classes of molecules that may afford new imaging agents, peptides are attractive as they often exhibit high affinity and high specificity for many pathogenic targets while large numbers of peptides are obtained combinatorially for screening.<sup>[2]</sup> Of several useful β<sup>+</sup>-emitting nuclides for PET, <sup>18</sup>F is a mainstay owing to its excellent nuclear properties and on-demand production at Curie levels or higher in hospital cyclotrons. Nevertheless, considerable challenges persist for labeling peptides with [<sup>18</sup>F]fluoride ion:<sup>[3]</sup> in water fluoride ion is a poor nucleophile<sup>[4]</sup> whereas peptides and other large biomolecules are solubilized in water. Because of this incompatibility, <sup>18</sup>F-labeling often requires several steps starting with at least one drying step followed by the synthesis of an <sup>18</sup>F-radioprosthetic group that is conjugated to the peptide in at least one additional step.<sup>[5]</sup> While multistep procedures are common, they are challenged by the relatively short half-life of <sup>18</sup>F (*t*<sub>1/2</sub> = 109.8 min) as well as the realization that each additional step reduces yields and increases the risk of radiosynthetic failure. To address these issues several one-step labeling methods have been reported.<sup>[6]</sup> However, to date, azeotropic drying is usually

required to concentrate, if not dry the [<sup>18</sup>F]fluoride ion to ensure high radiochemical yield.

Furthermore, following labeling, time-consuming HPLC purification is often required to remove unlabeled precursor so as to achieve (radio)chemical purity and ensure high specific activity e.g. >1 Ci μmol<sup>-1</sup>. Although a few tracers have been produced without HPLC purification, radiolabeled products in such cases can be contaminated with unlabeled byproducts which reduce the effective specific activity. Ideally, an <sup>18</sup>F-labeling method should supply a tracer in high purity, at high specific activity, and in an operationally simple manner that obviates both drying before synthesis and HPLC purification following. Moreover, bioconjugation should be user-friendly and amenable to various biomolecules for functional imaging. Hence the prosthetic group should be small in size with no net charge to ensure that the tracer's properties are similar to those of the unlabeled analogue. A review of the vast literature on <sup>18</sup>F-labeling/PET imaging leads us to articulate the following attributes for ideal production of <sup>18</sup>F-PET tracers:

1. One-step radiosynthesis without drying the [<sup>18</sup>F]fluoride ion;
2. No HPLC purification;
3. Good radiochemical yield (>25 %), high purity (>98 %), and high specific activity (>1 Ci μmol<sup>-1</sup>);
4. The <sup>18</sup>F-radioprosthetic group is small, free of charge, and stable in vivo;
5. Bioconjugation should be easy and provide precursors that can be stocked for on-demand use;
6. Labeled tracers based on different biomolecules should afford PET images of in vivo targets.

Working towards this ideal, we labeled [<sup>18</sup>F]-aryltrifluoroborate bioconjugates at very high specific activity in good radiochemical yields in 15 min.<sup>[7]</sup> Yet our previous reports fell slightly short of these ideals: HPLC purification was needed and in one case in vivo stability could be questioned.<sup>[8]</sup> To rectify these problems and bring us closer to an ideal radiolabeling method as described above, we now report a new zwitterionic alkylammoniomethyltrifluoroborate (AMBF<sub>3</sub>) that affords greatly improved attributes for radio-tracer development. These include: 1) in vitro and in vivo stability, 2) facile labeling by <sup>18</sup>F–<sup>19</sup>F isotope exchange (IEX),<sup>[9]</sup> 3) HPLC-free purification, 4) synthetic and radio-synthetic simplicity, and 5) in vivo images of several tumor targets. In developing this method we also describe an efficient method for eluting fluoride ion that delivers Curie levels of [<sup>18</sup>F]fluoride ion within roughly 60 μL saline (>15 mCi μL<sup>-1</sup>) such that concentration by drying may be

[\*] Z. Liu, M. A. Radtke, Prof. Dr. D. M. Perrin  
Chemistry Department, University of British Columbia  
2036 Main Mall, Vancouver, BC, V6T-1Z1 (Canada)  
E-mail: dperrin@chem.ubc.ca

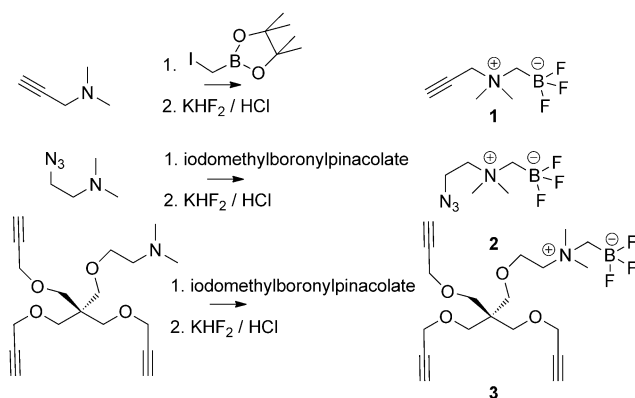
M. Pourghiasian, J. Lau, Dr. J. Pan, Dr. K.-S. Lin, Prof. Dr. F. Bénard  
Experimental Therapeutics, B.C. Cancer Research Agency  
675 West 10th Avenue, Vancouver, BC, V5Z-1L3 (Canada)  
G. M. Dias, Dr. D. Yapp  
Molecular Oncology, B.C. Cancer Research Agency  
675 West 10th Avenue, Vancouver, BC, V5Z-1L3 (Canada)

[\*\*] This work was supported by NSERC and by CCSRI Grant no 20071 and by an SOF grant from Genome B.C.

Supporting information for this article is available on the WWW under <http://dx.doi.org/10.1002/anie.201406258>.

avoided. We validate this labeling method with preliminary PET images of several new tracers ranging from small-molecule trimers to large peptide dimers and trimers. Given the urgent need for new tracer development, this method is likely to provide a rapid entry into  $^{18}\text{F}$ -radiotracers, particularly for peptides and other molecules.

The  $\text{AMBF}_3$  moiety was designed based on an unexpected observation: the solvolytic rate constant of a given non-aromatic organotrifluoroborate ( $k_{\text{sol.v.}}$ ) is highly correlated with the  $\text{p}K_{\text{a}}$  of the corresponding carboxylic acid; to wit, butyl- $\text{BF}_3^-$  solvolyzes rapidly ( $k_{\text{sol.v.}} = 0.3 \text{ min}^{-1}$ ) as the  $\text{p}K_{\text{a}}$  of butyric acid is 4.7, while  $\text{AMBF}_3$  solvolyzes slowly ( $k_{\text{sol.v.}} = 3.1 \cdot 10^{-5} \text{ min}^{-1}$ ) as the  $\text{p}K_{\text{a}}$  of betaine is 1.8.  $\text{AMBF}_3$  is readily prepared by alkylating a tertiary amine (see Scheme 1) and hence affords considerable synthetic simplicity for bioconjugation. Furthermore, in contrast to relatively bulky aryltrifluoroborates, it is relatively small in size.



**Scheme 1.** Synthesis of radiosynths **1–3** via amine alkylation with iodomethylboronylpinacolate followed by conversion to the zwitterionic  $\text{AMBF}_3$ .

Iodomethylboronyl pinacolate was treated with three different functionalized *N,N*-dimethylamines to give the quaternary ammoniomethylboronyl pinacolates in high yield (see the Supporting Information).<sup>[10]</sup> Pure trifluoroborates are obtained following reaction in acidic  $\text{KHF}_2$  as shown in Scheme 1. Propargyl- $\text{AMBF}_3$ , **1**, and azidoethyl- $\text{AMBF}_3$ , **2**, are obtained. A tris-propargylether derivative of pentaerythritol with a pendant tertiary amine was condensed similarly to afford **3**, which enables production of dual-mode fluorescent peptide tracers and trimeric tracers (see below).  $^{19}\text{F}$  NMR spectroscopy confirmed extremely slow solvolysis of compound **1**:  $t_{1/2}$ :  $13 \pm 0.3$  days (see the Supporting Information). Radiosynths **1–3** undergo Cu-catalyzed dipolar cycloaddition reactions that have been used extensively for conjugation to peptides, enzyme inhibitors, and other functional small molecules.<sup>[11]</sup>

For labeling, a wet NCA (no carrier added) solution of  $^{18}\text{F}$ fluoride ion is used directly following trapping. Using disposable labware, we affixed a very small QMA cartridge (9 mg resin) to the reaction vessel (10 mL polypropylene conical tube), as shown in Figure 1. The very small QMA column efficiently traps Curie levels of NCA  $^{18}\text{F}$ fluoride ion,

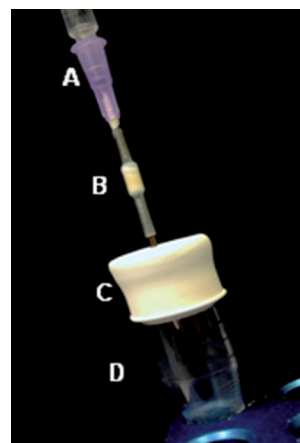


**Figure 1.** NCA  $^{18}\text{F}$ fluoride ion elution trap. A: 16-gauge needle where the needle has been cut; B: anion-exchange cartridge containing 9 mg of standard QMA resin fitted with the remaining needle point; C: standard rubber septum; D: in temp block: polypropylene vial (sawed-off Falcon tube) that contains  $\text{AMBF}_3$  precursor. NCA  $^{18}\text{F}$ fluoride ion is trapped on the cartridge, which is then inserted into the septum. The  $^{18}\text{F}$ fluoride ion is eluted with 60  $\mu\text{L}$  isotonic saline into the tube D in which labelling proceeds. All events occur within a fully shielded hot-cell.

which are directly eluted with  $< 60 \mu\text{L}$  saline ( $> 95\%$  recovery,  $n = 50$ ) into the reaction vessel containing  $\text{AMBF}_3$ -bioconjugates to be labeled by IEX (see below).

In order to accurately measure high specific activity while demonstrating radiochemical purity in an HPLC-free radiosynthesis, we conjugated **2** to alkyne-rhodamine (568 nm,  $\epsilon = 100\,000 \text{ M}^{-1} \text{ cm}^{-1}$ ) to give a prototypical dual-mode fluorescent PET tracer:  $\text{AMBF}_3$ -rhodamine (**4a**, see Figure 4), which was stored in lyophilized aliquots of 45  $\mu\text{g}$  ( $\approx 50 \text{ nmol}$ ). For labeling, one aliquot was dissolved in 50% DMF/water (40  $\mu\text{L}$ , pH 2.5 buffer) and transferred to the polypropylene tube into which NCA  $^{18}\text{F}$ fluoride ion (780–1000 mCi) was eluted. Once mixed (10 s), the vial was placed in a heating block at  $80^\circ\text{C}$ . After 15 min, the reaction was quenched with 2 mL PBS or 2 mL  $\text{NH}_4\text{OH}$  and the entire reaction mixture was directly loaded onto a C18 Sep-Pak column. Following water wash (5 mL) the tracer was eluted into PBS/ethanol (2 mL). In general, starting with roughly 1 Ci NCA  $^{18}\text{F}$ fluoride ion,  $^{18}\text{F}$ **4a** was obtained in decay-corrected radiochemical yields of  $25 \pm 4.5\%$  ( $n > 20$ ) in 25 min. HPLC analysis confirmed purity, which shows only one peak in the radioactive and visible (568 nm) modes (Figure 2). As approximately 200 mCi radiolabeled tracer was obtained starting with 50 nmol precursor, the specific radioactivity was  $4 \text{ Ci } \mu\text{mol}^{-1}$ , a value that is expected to be at least adequate, if not high for most applications. This value was verified by a standard curve (see the Supporting Information) that showed that specific activity is indeed  $3\text{--}4 \text{ Ci } \mu\text{mol}^{-1}$  ( $n \geq 3$ ).

In contrast to previously reported  $^{18}\text{F}$ ArBF<sub>3</sub> compounds where about 50% of the  $\text{ArBF}_3$  may hydrolyze to the  $\text{ArB}(\text{OH})_2$  during the IEX reaction,<sup>[7a,d]</sup> here no boronic acid is detected due to the much greater solvolytic stability of the  $\text{AMBF}_3$ . Hence, HPLC purification can be replaced with a simple reverse-phase Sep-Pak elution that provides tracer in

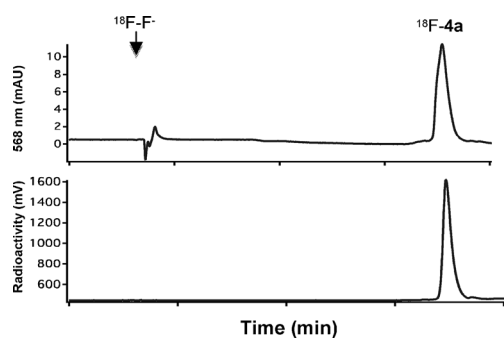


**Figure 2.** Reverse-phase HPLC traces of [ $^{18}\text{F}$ ]AMBF $_3$ -rhodamine with UV/Vis absorbance (top) and radioactivity detection (bottom).

> 95 % purity. In terms of stability, AMBF $_3$ -rhodamine shows negligible decomposition in serum after 150 min at 37°C (Figure 3), which is consistent with the very long solvolytic half-life observed by  $^{19}\text{F}$  NMR spectroscopy. We then verified the in vivo stability of [ $^{18}\text{F}$ ]4a in mice.

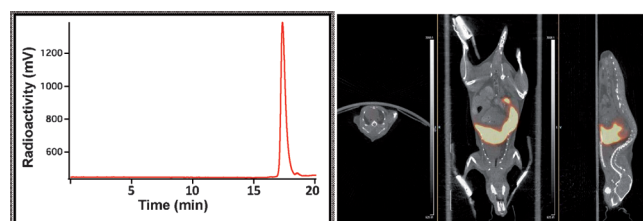


**Figure 3.** Left: Reverse-phase radio-HPLC trace following incubation of [ $^{18}\text{F}$ ]AMBF $_3$ -rhodamine in mouse plasma for 150 min. Right: Representative PET/CT image at 60 min.

[ $^{18}\text{F}$ ]4a accumulated in mitochondria-rich organs such as the liver and heart, as seen with other  $^{18}\text{F}$ -rhodamine tracers. Minimal uptake in other organs was detected, most notably bone, wherein accumulation was less than 0.5 % ID/g. Not surprisingly, [ $^{18}\text{F}$ ]AMBF $_3$  appears to be metabolically stable as the anionic BF $_3^-$  group is noncoordinating and bioorthogonal. Because [ $^{18}\text{F}$ ]4a is not expected to bind a specific target, Figure 3 simply shows in vivo stability and an absence of bone uptake. In order to validate this method for imaging specific targets, we conjugated **1** or **3** to several molecularly complex peptidic ligands of clinical interest (Figure 4). These were then labeled (see the Supporting Information) and imaged (see Figure 5).

Among them, [ $^{18}\text{F}$ ]AMBF $_3$ -octreotate (**4b**) was designed for imaging the somatostatin-type-2 receptor (sstr2). Octreotate is an sstr2 agonist that has been labeled with  $^{18}\text{F}$ ,  $^{68}\text{Ga}$ ,  $^{64}\text{Cu}$ ,  $^{111}\text{In}$ , and  $^{99\text{m}}\text{Tc}$  in a clinical setting to image sstr2-positive neuroendocrine tumors.<sup>[12]</sup> Compound **4b**, prepared by simple conjugation of octreotate-azide to **1**, was labeled within 30 min in yields of roughly 30 % and at > 3 Ci  $\mu\text{mol}^{-1}$  with high uptake (> 10 % ID/g) in AR42J pancreatic tumor xenografts along with blocked controls (data not shown), a very high tumor-to-muscle ratio of > 80, and especially rapid clearance with minimal uptake in liver.<sup>[13]</sup> Indeed, this

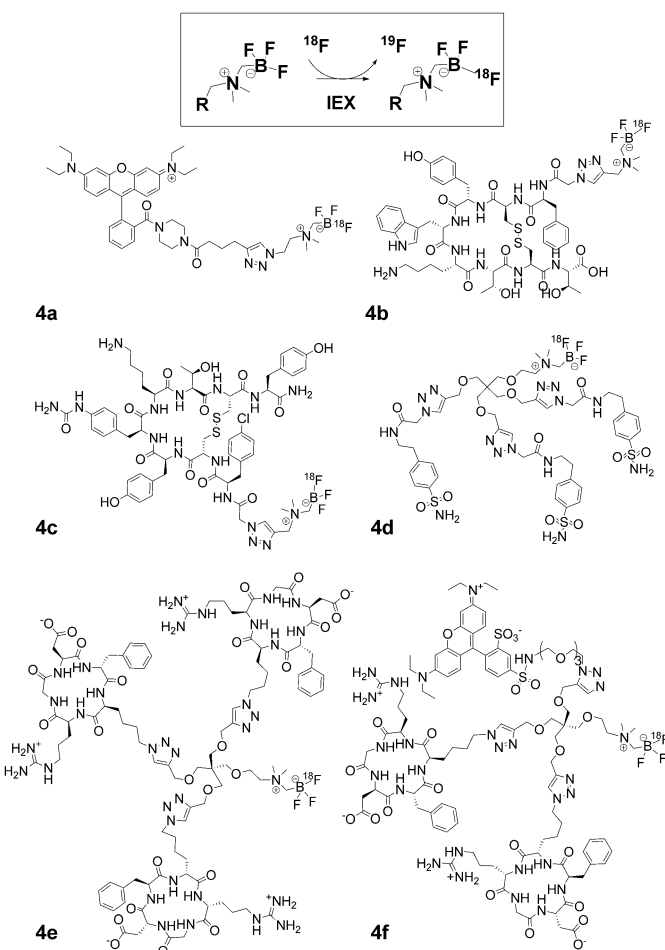


**Figure 4.** AMBF $_3$ -bioconjugates: **4a** (rhodamine), **4b** (octreotate), **4c** (LM3: a somatostatin receptor antagonist), **4d** (a trimeric carbonic anhydrase inhibitor), **4e** (trimeric RGD) and **4f** (dual-mode fluorescent-dimeric RGD).

represents a significant improvement over other  $^{18}\text{F}$ -labeled octreotates. To extend this method to an sstr2 antagonist, we conjugated **1** to an octreotate analogue to give **4c** (AMBF $_3$ -LM3). Labeling gave radiochemically pure [ $^{18}\text{F}$ ]4c (ca. 200 mCi) in 20 min in comparable yields at high specific activity (ca. 3 Ci  $\mu\text{mol}^{-1}$ ). [ $^{18}\text{F}$ ]4c also showed specific and very high tumor uptake in AR42J pancreatic xenograft tumors in mice. Unbound tracer cleared rapidly through the kidneys with minimal uptake in liver and negligible uptake in bone.

Next, we hypothesized that **3** could be conjugated to non-peptidic small-molecule enzyme inhibitors. Carbonic anhydrase-IX (CA-IX) is a surrogate marker for hypoxia and a promising diagnostic/therapeutic target for cancers.<sup>[14]</sup> Whereas sulfonamide derivatives are known to inhibit CA-IX, as far as we know, there are very few examples of successful PET probes that have been developed based on CA-IX inhibitors. Here **3** provided a ready entry into a multivalent small-molecule tracer **4d**. Because of its polarity and higher molecular weight, it does not cross the erythrocyte cell membrane to bind to cytosolic CA-I or CA-II. This significantly reduces the background uptake and improves

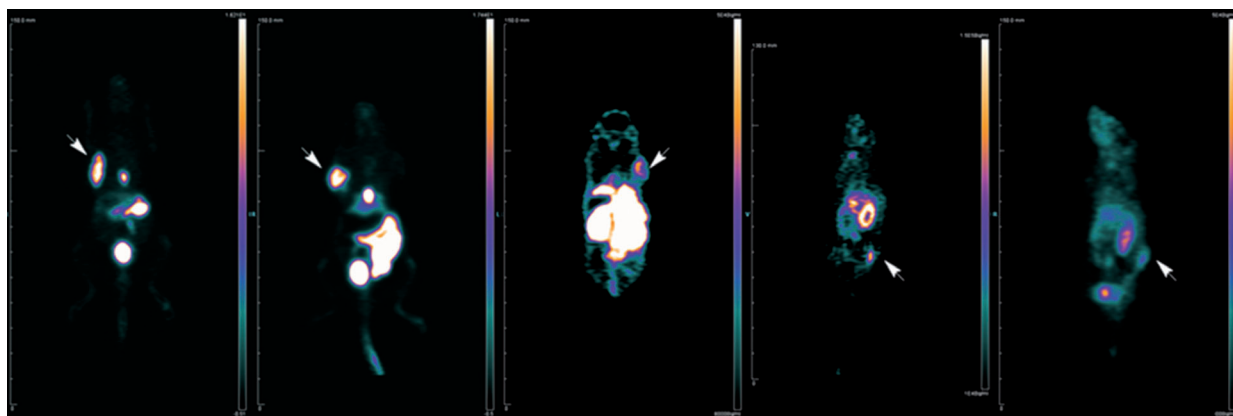


**Figure 5.** Representative PET images of  $^{18}\text{F}$ -labeled **4b**, **4c**, **4d**, **4e**, and **4f** (from left to right). The tumor is indicated by white arrow in each image. The PET images were reconstructed at 60 min post-injection.

image contrast. Precursor **4d** was radiolabeled in kit-like manner in comparable yields within 25 min with  $>99\%$  radiochemical purity and at roughly  $3\text{ Ci }\mu\text{mol}^{-1}$ . CA-IX-expressing HT29 tumor xenografts were imaged by  $^{18}\text{F}$ -**4d** and clearly visible as early as 20 min post-injection. Although this tracer will require further synthetic modification to reduce gastrointestinal uptake, these preliminary images demonstrate the first successful  $^{18}\text{F}$ -PET imaging of CA-IX target, which highlights a promising strategy to trimerize small inhibitors as  $^{18}\text{F}$ -radiotracers.

On account of an enduring clinical interest in RGD peptides<sup>[5,15]</sup> we used **3** to conjoin either three cycloRGD moieties (**4e**) in one step, and to prepare a dual-mode tracer (**4f**) by first linking **3** to rhodamine followed by two cycloRGD moieties. To cleanly graft a single fluorophore, a large excess of **3** was reacted in the presence of limiting rhodamine-azide while unreacted **3** was recycled. Radiochemical yields and specific activities were comparable to other tracers (see the Supporting Information). Representative PET images are shown in Figure 5; uptake values in U87M glioblastoma xenografts were roughly  $1.8\%$  ID/g for  $^{18}\text{F}$ -**4e** and  $5.5\%$  ID/g for  $^{18}\text{F}$ -**4f**. Interestingly, the dual-mode tracer (**4f**) with both fluorescent and PET properties showed higher tumor uptake, which suggests that a fluorophore can be used to improve tumor uptake while providing fluorescent detection on cells and in tumor tissues.<sup>[16]</sup>

Overall, tumor uptake values vary from extraordinarily high to low:  $^{18}\text{F}$ -**4b** provides some of the highest tumor uptake values and T:NT (tumor/non-tumor) ratios of any labeled octreotate, irrespective of isotope or prosthesis, whereas in the case of  $^{18}\text{F}$ -**4e** and  $^{18}\text{F}$ -**4f**, tumor uptake values were lower. Yet uptake is known to be variable because it is a complex function of target affinity, dissociation rates, and clearance rates, phenomena which in turn depend on the ligand, the prosthetic group, and the linker arm. Indeed, all tracers must be fine-tuned through synthetic iteration to modulate clearance.<sup>[17]</sup> Yet before linker arms and other modifications are introduced to improve image quality, it is paramount that a radioprosthetic group be identified that affords both convenient radiolabeling as well as the potential for excellent tumor uptake. Given the very high tumor uptake

values with  $^{18}\text{F}$ -**4b** and  $^{18}\text{F}$ -**4c**, along with the lack of bone uptake in all images, AMBF<sub>3</sub> provides a promising lead for tracer design.

Whereas radiosynthons **1–3** were designed for copper-catalyzed azide–alkyne cycloaddition (CuAAC) conjugation, secondary/tertiary amines, tertiary phosphines, as well as thioethers, on various bioactive molecules may be alkylated for eventual labeling, or then conjugated to peptides by other methods, for example, NHS, maleimides etc. Labeling proceeds within a fully shielded hot-cell to provide multiple human tracer doses in high radiochemical purity and at high specific activity using simple disposable labware. This method should be easily adapted to a synthesis module as well as microfluidic reactors. In comparison to previously reported aryl- $^{18}\text{F}$ BF<sub>3</sub> compounds, the AMBF<sub>3</sub> shows great stability during labeling. As decomposition is negligible, no HPLC purification is required. Only a C18 Sep-Pak column is required for purification. As neither toxic metals nor chlorinated solvents are used in labeling, this method constitutes a “green” radiosynthesis.

Because labeling proceeds under acidic conditions, certain acid-sensitive linkages may not survive this method. Inasmuch as peptides are typically subjected to conditions that are substantially more acidic than those used herein (e.g. deprotection in  $80\%$  TFA, pH  $-2$ , purification in  $0.5\text{--}1\%$  TFA, pH  $0\text{--}1$ ) most peptides are likely to be labeled by this method. For very acid-sensitive biomolecules, one-pot two-step approaches can be contemplated.<sup>[8]</sup>

In summary, AMBF<sub>3</sub>, a new radiosynthon, is readily installed by simply alkylating an amine with iodomethylboron pinacolate, followed by KHF<sub>2</sub> treatment. A very small  $9\text{ mg}$  QMA column enables fluoride ion elution in small volumes often without need for an azeotropic concentration procedure, whereas IEX obviates HPLC purification because starting material and labeled product are chemically identical. Given the broad applications of CuAAC reactions, AMBF<sub>3</sub> was featured on radiosynthons for use with CuAAC. Synthon **3** provides for a dual-mode dimeric tracer as well as trimeric tracers. All conjugates are labeled in good yield and at high specific activity in near-record rapidity:  $<30\text{ min}$  (including  $^{18}\text{F}$ -isolation, labeling, and Sep-Pak purification). Full publi-



cations that detail tumor uptake values, time–activity curves, target affinities, and biodistribution data for **4b–4f**, along with several other clinically important peptides will be presented in the near future. In the meantime, we hope to share this method, embodied by AMBF<sub>3</sub> and its improved radiosynthetic ease and general utility, with others seeking to develop <sup>18</sup>F-tracers, especially peptides.

### Experimental Section

For labeling, precursor (**4a–4f**, 50–75 nmol), was resuspended in aqueous pyridazine/HCl buffer (pH 2.5) (ca. 50 µL) in a polypropylene (Falcon) tube. NCA [<sup>18</sup>F]fluoride ion (0.8–1 Ci), obtained by bombardment of H<sub>2</sub><sup>18</sup>O with 18 MeV protons, followed by anion-exchange resin trapping (9 mg, QMA, chloride ion form, washed with 1 mL distilled water), was eluted with PBS (ca. 60 µL) into the tube containing precursor. The tube was placed in a heating block at 80 °C for 12 min. In some cases, the reaction vessel was evacuated as previously reported.<sup>[7c]</sup> The reaction was quenched by NH<sub>4</sub>OH (5 % in water, 2 mL) or PBS (2 mL). The reaction mixture was loaded onto a C18 light cartridge which was washed with water (2 × 4 mL). Radiochemically pure product was eluted with 1:1 ethanol/saline (0.5 mL) into a glass vial to provide ≈200 mCi tracer, total time: 25 min. The tracer was formulated in isotonic saline (5 mL). A small sample was removed for quality-control analysis by HPLC. Detailed experimental procedures for synthesis, specific activity measurements, HPLC traces, are presented in the Supporting Information.

Received: June 16, 2014

Published online: September 4, 2014

**Keywords:** <sup>18</sup>F-labeling · bioconjugation · click chemistry · peptides · PET imaging

- [1] a) L. S. Cai, S. Y. Lu, V. W. Pike, *Eur. J. Org. Chem.* **2008**, 2853–2873; b) R. Y. Tsien, *Nat. Cell Biol.* **2003**, Ss16–Ss21; c) E. L. Cole, M. N. Stewart, R. Littich, R. Hoareau, P. J. H. Scott, *Curr. Top. Med. Chem.* **2014**, *14*, 875–900.
- [2] a) C. J. Hipolito, H. Suga, *Curr. Opin. Chem. Biol.* **2012**, *16*, 196–203; b) Q. C. Xu, K. S. Lam, *J. Biomed. Biotechnol.* **2003**, 257–266; c) X. Y. Li, D. R. Liu, *Angew. Chem. Int. Ed.* **2004**, *43*, 4848–4870; *Angew. Chem.* **2004**, *116*, 4956–4979; d) G. Smith, L. Carroll, E. O. Aboagye, *Mol. Imag. Biol.* **2012**, *14*, 653–666; e) M. K. J. Gagnon, S. H. Hausner, J. Marik, C. K. Abbey, J. F. Marshall, J. L. Sutcliffe, *Proc. Natl. Acad. Sci. USA* **2009**, *106*, 17904–17909; f) O. H. Aina, R. W. Liu, J. L. Sutcliffe, J. Marik, C. X. Pan, K. S. Lam, *Mol. Pharm.* **2007**, *4*, 631–651; g) L. Halab, F. Gosselin, W. D. Lubell, *Biopolymers* **2000**, *55*, 101–122.
- [3] H. C. Cai, P. S. Conti, *J. Labelled Compd. Radiopharm.* **2013**, *56*, 264–279.
- [4] C. G. Zhan, D. A. Dixon, *J. Phys. Chem. A* **2004**, *108*, 2020–2029.
- [5] F. T. Chin, B. Shen, S. L. Liu, R. A. Berganos, E. Chang, E. Mittra, X. Y. Chen, S. S. Gambhir, *Mol. Imag. Biol.* **2012**, *14*, 88–95.
- [6] a) C. Wängler, S. Niedermoser, J. S. Chin, K. Orchowski, E. Schirmacher, K. Jurkschat, L. Iovkova-Berends, A. P. Kostikov, R. Schirmacher, B. Wängler, *Nat. Protoc.* **2012**, *7*, 1946–1955; b) P. Laverman, C. A. D'Souza, A. Eek, W. J. McBride, R. M. Sharkey, W. J. G. Oyen, D. M. Goldenberg, O. C. Boerman, *Tumor Biol.* **2012**, *33*, 427–434.
- [7] a) Z. Liu, Y. Li, J. Lozada, K.-S. Lin, P. Schaffer, D. M. Perrin, *J. Labelled Compd. Radiopharm.* **2012**, *55*, 491–497; b) Z. Liu, N. Hundal-Jabal, M. Wong, D. Yapp, K. S. Lin, F. Benard, D. M. Perrin, *MedChemComm* **2014**, *5*, 171–179; c) Z. B. Liu, Y. Li, J. Lozada, P. Schaffer, M. J. Adam, T. J. Ruth, D. M. Perrin, *Angew. Chem. Int. Ed.* **2013**, *52*, 2303–2307; *Angew. Chem.* **2013**, *125*, 2359–2363; d) Z. Liu, Y. Li, J. Lozada, M. Q. Wong, J. Greene, K.-S. Lin, D. Yapp, D. M. Perrin, *Nucl. Med. Biol.* **2013**, *40*, 841–849; e) Y. Li, Z. B. Liu, J. Lozada, M. Q. Wong, K. S. Lin, D. Yapp, D. M. Perrin, *Nucl. Med. Biol.* **2013**, *40*, 959–966.
- [8] Y. Li, Z. Liu, M. Pourghiasian, K.-S. Lin, P. Schaffer, F. Benard, D. M. Perrin, *Am. J. Nucl. Med. Mol. Imaging* **2013**, *3*, 57–70.
- [9] a) R. Schirmacher, G. Bradtmoller, E. Schirmacher, O. Thews, T. R. Chan, R. Hilgraf, V. V. Fokin, K. B. Sharpless, M. G. Finn, B. Waengler, C. M. Niemeyer, K. Jurkschat, *Angew. Chem. Int. Ed.* **2006**, *45*, 6047–6050; *Angew. Chem.* **2006**, *118*, 6193–6197; b) Z. B. Li, K. Chansaenpak, S. L. Liu, C. R. Wade, P. S. Conti, F. P. Gabbai, *MedChemComm* **2012**, *3*, 1305–1308.
- [10] D. S. Matteson, D. Majumdar, *J. Organomet. Chem.* **1979**, *170*, 259–264.
- [11] a) V. V. Rostovtsev, L. G. Green, V. V. Fokin, K. B. Sharpless, *Angew. Chem. Int. Ed.* **2002**, *41*, 2596–2599; *Angew. Chem.* **2002**, *114*, 2708–2711; b) P. Wu, M. Malkoch, J. N. Hunt, R. Vestberg, E. Kaltgrad, M. G. Finn, V. V. Fokin, K. B. Sharpless, C. J. Hawker, *Chem. Commun.* **2005**, 5775–5777; c) Q. Wang, T. R. Chan, R. Hilgraf, V. V. Fokin, K. B. Sharpless, M. G. Finn, *J. Am. Chem. Soc.* **2003**, *125*, 3192–3193.
- [12] D. J. Kwekkeboom, B. L. Kam, M. van Essen, J. J. M. Teunissen, C. H. J. van Eijck, R. Valkema, M. de Jong, W. W. de Herder, E. P. Krenning, *Endocr.-Relat. Cancer* **2010**, *17*, R53–R73.
- [13] Z. Liu, M. Pourghiasian, F. Bénard, J. Pan, K.-S. Lin, D. M. Perrin, *J. Nucl. Med.* **2014**, DOI: 10.2967/jnumed.114.137836.
- [14] a) A. B. Stillebroer, P. F. A. Mulders, O. C. Boerman, W. J. G. Oyen, E. Oosterwijk, *Eur. Urol.* **2010**, *58*, 75–83; b) S. M. Monti, C. T. Supuran, G. De Simone, *Curr. Med. Chem.* **2012**, *19*, 821–830.
- [15] S. Maschauer, R. Haubner, T. Kuwert, O. Prante, *Mol. Pharm.* **2014**, *11*, 505–515.
- [16] Unpublished results.
- [17] S. Liu, *Bioconjugate Chem.* **2009**, *20*, 2199–2213.